Translational diffusion of fluorescent probes on a sphere: Monte Carlo simulations, theory, and fluorescence anisotropy experiment

M. M. G. Krishna,[a] Ranjan Das, and N. Periasamy[b]
Department of Chemical Sciences, Tata Institute of Fundamental Research, Homi Bhabha Road, Colaba, Mumbai 400 005, India

Rajaram Nityananda[c]
Raman Research Institute, Bangalore 560 080, India

(Received 7 December 1999; accepted 25 February 2000)

Translational diffusion of fluorescent molecules on curved surfaces (micelles, vesicles, and proteins) depolarizes the fluorescence. A Monte Carlo simulation method was developed to obtain the fluorescence anisotropy decays for the general case of molecular dipoles tilted at an angle α to the surface normal. The method is used to obtain fluorescence anisotropy decay due to diffusion of tilted dipoles on a spherical surface, which matched well with the exact solution for the sphere. The anisotropy decay is a single exponential for $\alpha=0°$, a double exponential for $\alpha=90°$, and three exponentials for intermediate angles. The slower decay component(s) for $\alpha\neq 0$ arise due to the geometric phase factor. Although the anisotropy decay equation contains three exponentials, there are only two parameters, namely α and the rate constant, D_{tr}/R^2, where D_{tr} is the translational diffusion coefficient and R is the radius of the sphere. It is therefore possible to determine the orientation angle and translational diffusion coefficient from the experimental fluorescence anisotropy data. This method was applied in interpreting the fluorescence anisotropy decay of Nile red in SDS micelles. It is necessary, however, to include two other independent mechanisms of fluorescence depolarization for molecules intercalated in micelles. These are the wobbling dynamics of the molecule about the molecular long axis, and the rotation of the spherical micelle as a whole. The fitting of the fluorescence anisotropy decay to the full equation gave the tilt angle of the molecular dipoles to be $1\pm 2°$ and the translational diffusion coefficient to be $1.3\pm 0.1\times 10^{-10}$ m^2/s. © *2000 American Institute of Physics.* [S0021-9606(00)51619-5]

I. INTRODUCTION

Nanosecond and picosecond time-resolved fluorescence and anisotropy decay measurements provide important information about solvent–solute interactions and the rotational dynamics of the fluorophore in homogeneous media such as liquids.[1] The fluorescence techniques are widely used in complex systems such as heterogeneous and biological media but the interpretation of fluorescence data is not as straightforward as in liquids. For example, the fluorescence anisotropy decay of most dye molecules in liquids is single exponential,[1] and occasionally two exponentials.[2,3] On the other hand, the fluorescence anisotropy decay in heterogeneous or biological media is multiexponential. In liquids, the fluorescence anisotropy decay is not affected by the translational diffusion of the fluorophore. On the other hand, if the fluorophore is bound to the surface of a nanometer-size particle (micelles, vesicles, and proteins), the fluorescence is depolarized due to the translational diffusion of the dye on the surface as well. There are numerous experimental studies of fluorescence dynamics of fluorophores bound to micelles (nanometer size particles),[4–8] and surface diffusion was taken into account empirically in a few studies.[6–8] The theoretical and experimental studies on the fluorescence anisotropy decay of dipoles diffusing on curved cylindrical surfaces have been carried out.[9–11] Surprisingly, analytical equations for the anisotropy decay are not available for other curved surfaces, including the simple case of translational diffusion of fluorophores on a spherical surface.

In this work, a Monte Carlo simulation method has been developed for obtaining fluorescence anisotropy decay due to the translational diffusion of probes on curved surfaces in three dimensions. The anisotropy decay simulated for the diffusion of oriented dipoles on a spherical surface matched well with the analytical solution obtained by solving the diffusion equation for the same problem. The anisotropy equation is a three exponential function with slower decay components when the orientation of the dipole is away from the surface normal. A theoretical approach to this problem is also presented. The applicability of the equation to experimental anisotropy decay of Nile red in SDS micelle has been examined.

The problem of diffusion of probes on surfaces is important in many other areas of physical sciences such as nuclear magnetic resonance studies on micelles and membranes,[12–14] polymer dynamics and entanglement, etc.[15–18] The diffusion

[a]Present address: Department of Biochemistry and Biophysics, University of Pennsylvania School of Medicine, Philadelphia, PA 19104-6059.
[b]Author to whom correspondence should be addressed. Electronic mail: peri@tifr.res.in; fax: 091-22-215 2110/2181; phone: 091-22-215 2971/2979; ext. 2383.
[c]Present address: National Centre for Radio Astrophysics (NCRA), P.O. Box 3, Pune 411 007, India.

equations are necessary for understanding biological phenomena at a molecular level where the translational diffusion of solutes bound to different surfaces directly influence the rate of metabolism or the rate at which the chemical signals are conveyed.[14] The Monte Carlo method of solving translation diffusion on a curved surface described here can be extended to any regular or irregular surfaces and will be particularly useful in the case of systems that cannot be treated analytically.

II. METHODS

A. Diffusion on closed surfaces

Diffusion of a particle in space is a classical problem.[19] The diffusion equation for a particle confined to a surface in three dimensions is written as

$$\frac{\partial}{\partial t}P(x,y,z,t)=\left(\frac{\partial}{\partial x}\frac{\partial}{\partial y}\frac{\partial}{\partial z}\right)\overline{\overline{\mathbf{D}}}\begin{pmatrix}\frac{\partial}{\partial x}\\ \frac{\partial}{\partial y}\\ \frac{\partial}{\partial z}\end{pmatrix}P(x,y,z,t), \qquad (1)$$

where $P(x,y,z,t)$ is the probability of finding the diffusing particle at the coordinates x, y, z at time t. Here, $\overline{\overline{\mathbf{D}}}$, the diffusion coefficient, is a second rank tensor. When the surface is uniform, as in the case of problems studied here, one replaces the tensor $\overline{\overline{\mathbf{D}}}$ with an isotropic diffusion coefficient D, having the unit m^2/s. The above diffusion equation is sought to be solved for a given initial condition, namely, that the particle is located at x_0, y_0, z_0 at $t=0$, subject to appropriate boundary conditions to obtain the time dependent probability of finding the particle at any location on the surface. If the surface is a closed one, as in our case, the appropriate boundary condition is that at $t=\infty$, the probability of finding the particle at any location is equal to $1/A$, where A is the surface area. There are three methods for solving partial differential equations. The first and the best method is to solve exactly to obtain the mathematical equation. This is possible for regular surfaces, such as a sphere, ellipsoid, etc. The second method is to solve the equation by numerical methods. Numerical methods are widely used when the analytical solution cannot be obtained. The third method is to obtain the solution by Monte Carlo method which is essentially a simulation of the diffusion process itself. The last method can, in principle, be used to solve any diffusion problem and is particularly useful in the case of complicated curved surfaces where the diffusion equation cannot be setup under a convenient coordinate system or mathematically tedious to solve.

B. Monte Carlo simulations

The main theme of the Monte Carlo simulation[20] used in this study is to mimic the diffusion of the oriented molecular dipoles on curved three-dimensional surfaces and to obtain anisotropy decay due to depolarization on account of translational diffusion. In these simulations, the molecules were treated as point dipoles oriented at a particular angle with respect to the normal to the surface of the sphere. In this section, the mathematical operations for the simulation of multiple dipoles diffusing on a spherical surface are described. This method can be easily modified to simulate the translational diffusion on other curved surfaces based on the geometry of the surface. The simulation procedure is divided into three parts: selection of the initial distribution of the molecular dipoles, diffusion of the dipoles on the spherical surface, and calculation of the anisotropy function.

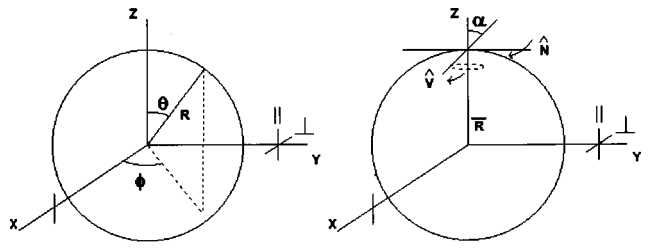

FIG. 1. (A) The figure shows the two polar angles θ and ϕ of a radial vector on the surface of a sphere with radius R in the xyz laboratory frame. The excitation light is polarized along the z-direction. The fluorescence anisotropy is calculated using the intensities along the parallel and perpendicular directions with respect to the polarization of the exciting laser beam. (B) This figure illustrates the selection of a random dipole vector $\hat{V}$ which makes an angle α with the radial vector $\overline{R}$ with the selection of a random normal vector $\hat{N}$. See text for details.

1. Selection of the initial distribution of the point dipoles

Let R be the radius of the sphere on which the dipoles are diffusing and D_{tr} be the translational diffusion coefficient. Let θ and ϕ be the standard polar angles of the dipole vector [Fig. 1(A)] and z be the axis which is coincident with the polarization of the exciting laser pulse. The initial distribution of the dipoles in the excited state was selected in the following steps. A distribution of ground state dipoles making an angle α with the respective radial vectors was selected such that the distribution of the dipoles is random over the entire spherical surface and the dipole orientation is random for the same angle α. Then the excited state distribution of the dipoles was obtained after ''excitation by a light pulse'' polarized in the z-axis, using the probability of excitation as $\cos^2\theta$. The distribution of excited state dipoles thus obtained will be identical to that in a real experiment.

The probability of a radial vector $\overline{R}$ making an angle θ with the z-axis is proportional to $\sin\theta$. This probability has to be satisfied during the selection of random radial vectors. A random number generator *ran2* (from ''Numerical Recipes in C''[21]) is used to generate real numbers distributed uniformly between 0 to 1. From these uniform deviates, the random numbers satisfying the required probability distribution, say, $P(\theta)$ (here $\sin\theta$), has to be generated. For this purpose, the ''Transformation Method''[20,21] was adopted. The method can be described briefly as follows. Let $p(x)$ represent the probability of the random numbers uniformly distributed between 0 and 1,

$$p(x)=1 \text{ for } 0\leqslant x\leqslant 1$$
$$=0 \text{ otherwise.} \tag{2}$$

The conservation of probability requires

$$\int_{x=-\infty}^{x} p(x)dx=\int_{\theta=-\infty}^{\theta} P(\theta)d\theta. \tag{3}$$

The above equation becomes

$$x=\int_{\theta=0}^{\theta} P(\theta)d\theta. \tag{4}$$

Therefore first a random number x between 0 to 1 was chosen, then the value of θ for which the area under the probability curve from 0 to θ is x times that of the total area under the probability curve was determined. The Cartesian coordinates of the radial vector was calculated from this θ value and a randomly selected ϕ value between 0 and 2π.

The dipole oriented at an angle α with respect to the radial vector $\overline{R}$ was obtained as follows. A random normal unit vector $\hat{N}$ perpendicular to the radial vector $\overline{R}$ was obtained such that $\overline{R}\cdot\hat{N}=0$. If (x_1,x_2,x_3) represent the components of $\overline{R}$ on the three Cartesian axes, then the components of the normal unit vector $\hat{N}$, (n_1,n_2,n_3) has to satisfy the two equations

$$x_1n_1+x_2n_2+x_3n_3=0 \tag{5}$$

and

$$n_1^2+n_2^2+n_3^2=1. \tag{6}$$

With the unit vector $\hat{N}=(n_1,n_2,n_3)$ as the axis of rotation, the radial vector $\overline{R}$ is rotated through the angle α to obtain a new vector $\overline{V}$ that is oriented at the angle α with the radial vector [Fig. 1(B)]. The rotation was done using the three-dimensional rotation matrix $D_{\hat{N}}(\alpha)$ which is given in Sec. II B 2. $\hat{V}$ is the unit vector along the dipole vector $\overline{V}$.

In selecting the normal unit vector $\hat{N}=(n_1,n_2,n_3)$ using Eqs. (5) and (6), random numbers were used such that the selected normal unit vectors are randomly distributed in the plane perpendicular to $\overline{R}$. This was done as follows. Initially, a specific normal vector was chosen depending on the values of the three components of the radial vector $\overline{R}=(r_1,r_2,r_3)$. If all the components of the radial vector are nonzero, then the normal vector chosen was $(-r_2,r_1,0)$. If some of the components are equal to zero, then the corresponding components of the normal vector are taken as one and for other components which are nonzero, the corresponding components were equated to zero. Using this specific normal vector and a randomly chosen angular variable ϕ_1 between 0 to 2π, the rotation matrix $D_{\hat{R}}(\phi_1)$ was used to rotate the specific normal vector through the angle ϕ_1 about the unit vector along the radial vector $\overline{R}$, to obtain the random normal vector in the plane perpendicular to the radial vector. The selection of random normal vectors to the radial vector makes sure that the dipole vectors are randomly oriented at the angle α with the respective radial vectors.

The probability of a dipole getting excited is proportional to $\cos^2\theta$, where θ is the angle made by the dipole with the z-axis. In selecting the excited dipoles with this probability, the same Transformation method described previously was adopted. A random number is chosen and if this random number matches with the fraction of the area under the probability curve with the total area, then that dipole was retained. Otherwise, the procedure was repeated from the initial step of selecting the ground state distribution.

2. Diffusion of the dipoles on the spherical surface

Let $\hat{V}$, $\overline{R}$ and $\hat{V'}$, $\overline{R'}$ represent the point dipole vector and corresponding radial vector before and after the diffusion in a single time step (one iteration in simulation). The diffusion length is the same in the case of radial vector and dipole vector in a single time step. So the diffusion of the dipoles on the spherical surface was performed by rotation of the radial and dipole vectors by the three-dimensional rotation matrix about a randomly chosen vector $\hat{n}$ normal to the radial vector. This random normal vector was chosen by the same procedure described in Sec. II B 1. If $\hat{n}\equiv(n_1,n_2,n_3)$ represent the unit normal vector which is the axis of rotation and β is the angle of rotation, then the three-dimensional rotation matrix $D_{\hat{n}}(\beta)$ is given as[22]

$$D_{\hat{n}}(\beta)=\begin{pmatrix} \cos\beta+(1-\cos\beta)n_1^2 & (1-\cos\beta)n_1n_2-n_3\sin\beta & (1-\cos\beta)n_1n_3+n_2\sin\beta \\ (1-\cos\beta)n_1n_2+n_3\sin\beta & \cos\beta+(1-\cos\beta)n_2^2 & (1-\cos\beta)n_2n_3-n_1\sin\beta \\ (1-\cos\beta)n_3n_1-n_2\sin\beta & (1-\cos\beta)n_3n_2+n_1\sin\beta & \cos\beta+(1-\cos\beta)n_3^2 \end{pmatrix}. \tag{7}$$

The angle of rotation β was obtained as follows. The probability of finding a particle at r at time t given that the initial position is r_0 at $t=0$ for diffusion on a two-dimensional infinitely planar surface[23] is given by

$$W(r,t;r_0,0)=\frac{1}{4\pi Dt}\exp\left(-\frac{|r-r_0|^2}{4Dt}\right), \tag{8}$$

where D is the diffusion coefficient. In the case of diffusion

on a spherical surface, the probability equation for the angle β at time t given that $\beta=0$ at $t=0$, is [Eq. (20) with proper normalization]

$$W(\beta)=\frac{1}{4\pi R^2}\Sigma_l(2l+1)P_l(\cos\beta)\exp\left(-\frac{l(l+1)D_{\rm tr}t}{R^2}\right). \tag{9}$$

Since this is an infinite sum of Legendre polynomials $P_l(\cos\beta)$, it is computationally intensive to calculate β. Hence, an approximate equation was used in the simulation procedure that is valid only for extremely small time scales. This was obtained from the probability equation for the planar diffusion [Eq. (8)] by replacing the displacement $|r-r_0|$ by $R\,\beta$ (β measured in radians). The probability of the angle of rotation β satisfies Eq. (10),

$$W(R\beta)\cong\frac{1}{4\pi D_{\rm tr}t}\exp\left(-\frac{R^2\beta^2}{4D_{\rm tr}t}\right). \tag{10}$$

The mean displacement $R\beta_m$ (where β_m is the mean angular displacement) per iteration is calculated as

$$R\beta_m=2\sqrt{D_{\rm tr}\tau}, \tag{11}$$

where τ is the time per iteration. It is important to note that the probability Eq. (10) is true only for very small τ and mean displacements. Hence the time per iteration τ is chosen appropriately such that this condition is valid. For example, for the values of $R=10$ Å and $D_{\rm tr}=1\times10^{-5}$ cm^2/s, the time per iteration τ is chosen as 1 ps such that the mean angular displacement $\beta_m\approx0.063$ rad.

The diffusion was carried out in two different ways. In the first method, the mean angular displacement β_m per iteration was calculated and this value was used as the angle of rotation β in one iteration. In the second method, the β values satisfying Eq. (10) ($t=\tau$) were calculated using the random numbers generated by the Transformation method described earlier. [It may be noted that the probability in the area element between β and $\beta+d\beta$ on the surface of the sphere is $2\pi R^2W(R\beta)\sin\beta d\beta$.] After getting a value for β and the randomly chosen unit normal vector components, the three-dimensional rotation matrix was computed. The new vectors $\hat{V'}$ and $\overline{R'}$ were then obtained by multiplying $\hat{V}$ and $\overline{R}$ with the matrix $D_{\hat{n}}(\beta)$. The anisotropy decays generated using these two methods are very similar.

The selection of the time step per iteration is important such that the mean displacement is very small compared to the radius itself and at the same time large enough such that the simulation of anisotropy decay is completed in a reasonable number of iterations. The number of iterations can be doubled to achieve the same level of anisotropy decay by reducing the iteration time by 4 or by reducing the diffusion coefficient by 4. Anisotropy decays were almost independent of iterations for $\beta_m<0.08$ rad.

3. Calculation of the anisotropy function

The ''fluorescence intensity'' along the x, y, and z-axes were calculated as squares of the respective components of the dipole vector $\hat{V}$. The components along x and y-axes ought to be quantitatively equal (except for simulation noise) which was used to check the algorithm. The anisotropy was calculated as

$$r(t)=\frac{I_\parallel-I_\perp}{I_\parallel+2I_\perp}=\frac{I_z-I_x}{I_x+I_y+I_z}=\frac{I_z-I_y}{I_x+I_y+I_z}. \tag{12}$$

The fluorescence anisotropy due to diffusion on the spherical surface ought to decrease to zero. Hence, the diffusion of the dipoles was continued until the anisotropy decreases to a value which is comparable to the accuracy ($<0.1\%$ of the initial value) in typical experiments.

The validity of each and every step in this simulation procedure was checked with the help of computer graphics. If the initial selection of excited dipoles follows $\cos^2\theta$ distribution, then the initial anisotropy r_0 value should be independent of the orientation angle α and should be equal to 0.4, which was observed. The selection of random normal vectors and the use of the rotation matrix $D_{\hat{n}}(\beta)$ in simulating the surface diffusion of dipoles were also tested. The simulation was done for varying values of α with about 85 000 dipoles diffusing on a spherical surface, using a DEC Alpha OSF/1 Computer system. The simulation was also carried out for varying values of radius of the sphere R and translational diffusion coefficient $D_{\rm tr}$. The results are discussed in Sec. III A.

C. Experiment

1. Materials

Nile red (Nile Blue A Oxazone, Exciton Inc., USA) and SDS (Sodium dodecyl sulfate, Sigma Chemical Co., USA), were used as received. The structure of the dye Nile red is shown in Fig. 2. The fluorescence decay of Nile red in ethanol was single exponential indicating the purity of the dye. The fluorescence lifetime of Nile red was 3.57 ns in ethanol. The 2% SDS micelle solution was prepared by stirring the surfactant in warm deionized water for about 1 h. The Nile red dye (in ethanol solution) was added and stirred. The dye (2.27 μM) to surfactant (0.069 M) ratio was $\approx$1:30 000.

2. Fluorescence measurements

The steady state fluorescence and anisotropy measurements were made using either Shimadzu RF540 or SPEX Fluorolog 1681 T format spectrofluorophotometers. The time resolved fluorescence measurements were made using a high repetition rate (800 kHz) picosecond dye laser (rhodamine 6G) coupled with a time correlated single photon counting

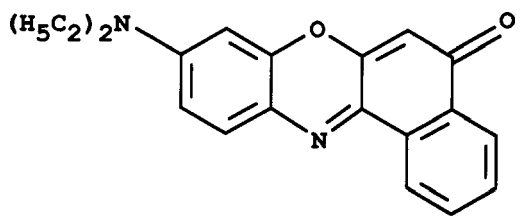

Nilered

FIG. 2. Structure of the dye Nile red.

(TCSPC) spectrometer described elsewhere,[24,25] currently using a microchannel plate photomultiplier (Hamamatsu 2809). The samples were excited at the excitation wavelength of 570 nm and the fluorescence decays were collected at the emission wavelength of 640 nm which is the emission maximum of Nile red in SDS micelles. The sample was excited with vertically polarized light and the fluorescence decay was collected with emission polarizer kept at the magic angle ($\approx 54.7°$) with respect to the excitation polarizer for measuring fluorescence lifetimes. For the anisotropy measurements, the fluorescence intensities were measured with the emission polarizer set at parallel or perpendicular orientation with respect to the excitation polarizer. Geometry factor (*G*-factor) for the TCSPC setup was determined by using the Nile red solution in ethanol whose rotational correlation time (0.18 ns) is faster than its fluorescence lifetime (3.57 ns). The emission of Nile red is completely depolarized after 2 ns. The parallel and perpendicular polarized components were collected for the times $t_{\|}$ and $t_{\perp}$ seconds such that the two decays overlap exactly in the tail region (after 2 ns). From these two values, *G*-factor is calculated as $t_{\perp}/t_{\|}$. For the case of Nile red in SDS micelles, the two polarized decays were collected for the times that are in the same ratio. The instrument response function (IRF) was recorded using a nondairy creamer scattering solution. The full width at half maximum (FWHM) of the IRF is about 150 ps. Typical peak count in the emission decay for fluorescence intensity and anisotropy measurements was about 200 000 and the total counts in the decay was typically 13 million. The time per channel was 37.84 ps.

The experimentally measured fluorescence decay data $F(t)$ is a convolution of IRF, $R(t)$ with the intensity decay function $I(t)$ according to the equation

$$F(t)=\int_0^t R(s)I(t-s)ds. \tag{13}$$

The intensity decay data was fitted to the appropriate equations by iterative deconvolution procedure using Levenberg–Marquardt algorithm for optimization of the parameters.[20,24,26,27] In the case of systems studied here, the fluorescence decay data was fitted to either a single (magic angle decay) or a multiexponential (polarized fluorescence decays) function as

$$I(t)=\Sigma_i \alpha_i \exp\left(-\frac{t}{\tau_i}\right), \tag{14}$$

where α_i and τ_i are the amplitudes and the lifetimes.

The polarized fluorescence decays (parallel and perpendicular) were usually fitted simultaneously (or globally) to appropriate functions defining the population decay (one or two lifetimes as determined by the decay at magic angle) and anisotropy decay, $r(t)$.[28–30] As will be noted elsewhere, the anisotropy decay of micelle-bound fluorophore is a multiplication of contributions from three independent depolarizing motions. For this reason it was decided to extract the best representation of $r(t)$ from experimental data rather than follow the conventional procedure (see below). For the calculation of the anisotropy decay, $r(t)$, one requires the polarized intensity decay functions $I_{\|}(t)$ and $I_{\perp}(t)$. The *G*-factor corrected polarized fluorescence decays [parallel and perpendicular, $F_{\|}(t)$ and $F_{\perp}(t)$] were individually fitted to a four exponential function to give a good fit to the experimental data. The good fits were judged by the randomness of residuals using the following criteria: (i) random distribution of residuals, (ii) value of chi-square (close to 1.0), and (iii) distribution of autocorrelation function values.[27] The purpose of these fits is to simply represent the intensity decay curves ($I_{\|}(t)$ and $I_{\perp}(t)$) and no physical meaning is attributed to the lifetimes and amplitudes obtained in the fits. Using these two intensity decay functions, the anisotropy decay is calculated using the equation

$$r(t)=\frac{I_{\|}(t)-I_{\perp}(t)}{I_{\|}(t)+2I_{\perp}(t)}. \tag{15}$$

This smoothly varying fluorescence anisotropy decay was used for the final testing of the theoretical equation.

The analysis of data described above uses a strategy in which $I_{\|}(t)$ or $I_{\perp}(t)$ are fitted to four exponentials even though $r(t)$ is a six exponential function. The numerical accuracy of this procedure was tested using simulated data. $I_{\|}(t)$ and $I_{\perp}(t)$ were calculated at the intervel of 40 ps up to 12 ns (300 points) for typical values for the parameters relevant to the problem of diffusion of the fluorophore (fluorescence lifetime 2.5 ns) in a micelle. $I_{\|}(t)$ and $I_{\perp}(t)$ are defined as follows:[30]

$$\begin{aligned} I_{\|}(t)&=\frac{1}{3}\exp\left(-\frac{t}{2.5\,\text{ns}}\right)[1+2r(t)],\\ I_{\perp}(t)&=\frac{1}{3}\exp\left(-\frac{t}{2.5\,\text{ns}}\right)[1-r(t)], \end{aligned} \tag{16}$$

where the anisotropy decay $r(t)$ is defined by Eq. (33). The following values were used for the calculation: $r(0)=0.4$, $\alpha=15°$, $\tau_{\text{tr}}=15$ ns, $\tau_w=1$ ns, $S=0.5$, and $\tau_m=10$ ns. $r(t)$ is a six exponential function and hence $I_{\|}(t)$ or $I_{\perp}(t)$ is a seven exponential function. For the above simulation values the time constants of the seven exponentials were 2.5, 1.2, 1.111, 0.75, 0.545, 0.526, and 0.429 ns. The amplitudes of seven exponentials were positive in $I_{\|}(t)$, whereas six of the amplitudes were negative in $I_{\perp}(t)$. It was found that $I_{\|}(t)$ could be fitted to a four exponential function with time constants 2.619, 2.372, 1.053, and 0.527 ns with positive amplitudes for all. The deviation of the fitted value from the true value, $(I_{\text{true}}-I_{\text{calc}})/I_{\text{true}}$, was less than 1×10^{-5}. Similarly, $I_{\perp}(t)$ could be fitted to a four exponential function with time constants 2.501, 1.130, 0.544, and 0.522 ns with negative amplitudes for the last three time constants. The deviation of the fitted value from the true value was less than 1×10^{-6}. The deviation of the difference $(I_{\|}(t)-I_{\perp}(t))$ from the true value was also less than 1×10^{-5}. We therefore conclude that the fitting procedure described above for obtaining numerical representations of $I_{\|}(t)$, $I_{\perp}(t)$, and $r(t)$ from the experimental data are satisfactory.

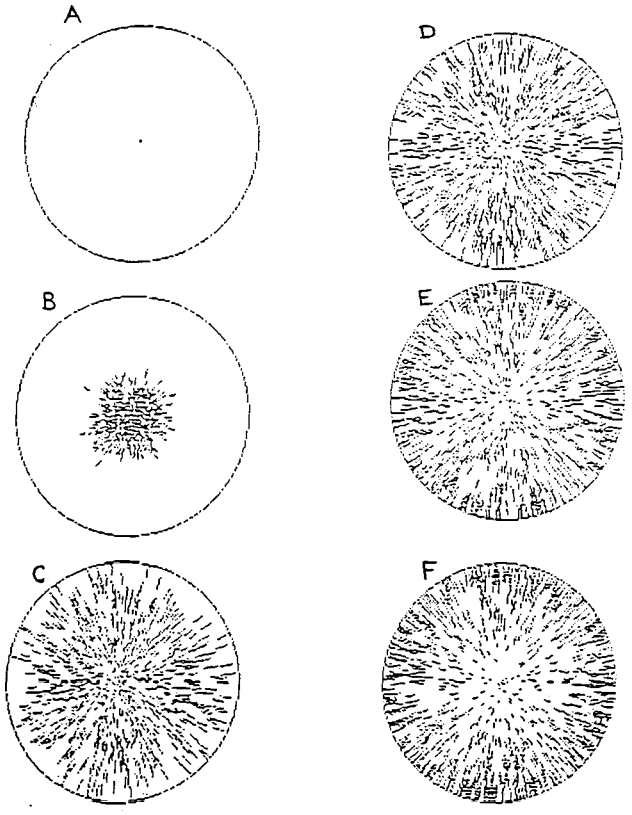

FIG. 3. Translational diffusion of the dipoles oriented along z-axis on the surface of the sphere, as viewed from above z-axis (projected in the xy-plane). (A)–(F) show the distribution of the dipoles on the surface of the sphere at different stages. The simulation parameters were radius of the sphere, $R=10$ Å, translational diffusion coefficient, $D_{tr}=1\times10^{-5}$ cm^2/s and time step per iteration, $\tau=1$ ps.

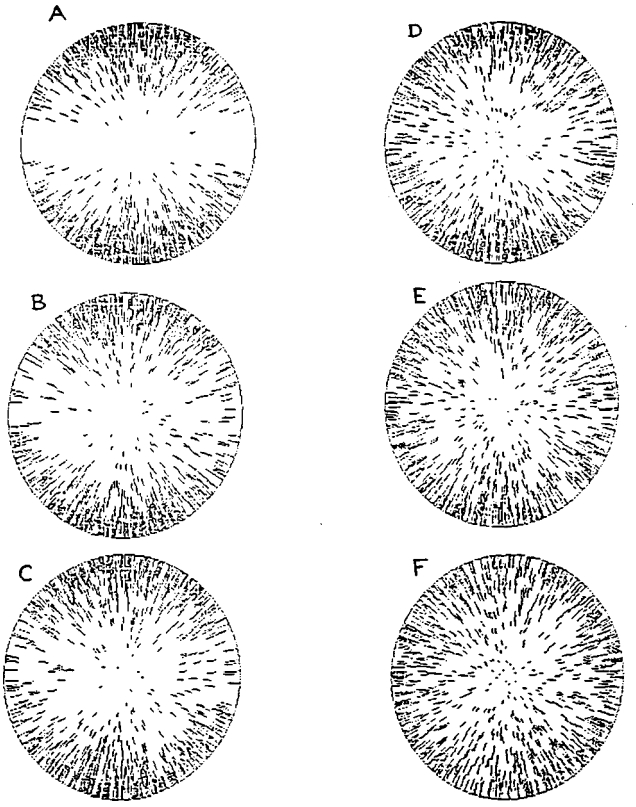

FIG. 4. Translational diffusion of the excited dipoles oriented along the radial vectors on the surface of the sphere as projected on the yz-plane. The excited dipoles are initially selected with the probability $\cos^2\theta$, where θ is the angle made with the z-axis which is the axis of polarization of the excitation light. (A)–(F) show the distribution of the dipoles on the surface of the sphere at different stages of the translational diffusion. The simulation parameters were radius of the sphere, $R=10$ Å, translational diffusion coefficient, $D_{tr}=1\times10^{-5}$ cm^2/s and time step per iteration, $\tau=1$ ps. The corresponding fluorescence anisotropy decay curve is shown in Fig. 5.

III. RESULTS AND DISCUSSION

A. Results of the Monte Carlo simulations

The translational diffusion of 85 000 excited dipoles oriented along the normal to the spherical surface ($\alpha=0$) is shown in Figs. 3 and 4 at different stages of the Monte Carlo simulation (refer the figure captions for details of simulation parameters). Figure 3 shows the surface diffusion for the case when all the dipoles are oriented parallel to the z-axis, to illustrate the random diffusion process modeled in the Monte Carlo simulations. Figure 4 shows the distributions for the case when the excited dipoles are initially distributed with the probability $\cos^2\theta$. The latter case is identical to the fluorescence anisotropy experiment using fluorophores embedded in spherical micelles. The components of intensities along the three axes, I_x, I_y, and I_z, and the anisotropy, $r(t)=(I_z-I_y)/(I_x+I_y+I_z)$, as a function of time are shown in Fig. 5. The anisotropy decay is identical for both the initial distributions except that $r(0)=1$ in the former case (Fig. 3) and $r(0)=0.4$ in the latter case (Fig. 4). The anisotropy decay is single exponential with the decay constant equal to $R^2/6D_{tr}$. The decay constant, $R^2/6D_{tr}$, is found to be independent of the value of R and D_{tr} used in the simulation as long as τ is chosen such that $\beta<0.1$. Single exponential decay is the one predicted by the theoretical equation for $\alpha=0$ (see below). The deviation of the simulated data from the exponential fit is shown in the bottom panel of Fig. 5.

The fluorescence anisotropy decays for the translational diffusion of dipoles tilted at an angle α (from 0° to 90°) with respect to the surface normal are shown in Fig. 6. These curves clearly show that the anisotropy decay depends on the orientation angle α. This is an unanticipated new result. All these decays can not be fitted to single exponential functions. At the extreme case of $\alpha=90°$, the anisotropy decay fits adequately to a double exponential function with the correlation times $R^2/6D_{tr}$ and $R^2/2D_{tr}$ and the respective amplitudes 0.25 and 0.75. It was not possible to fit the anisotropy decays at other α values to two exponential functions with the two correlation times fixed at these values. The fits were particularly bad at the intermediate values of α. The combined analysis of all the anisotropy decays at the seven values of α to a three exponential function with common correlation times (and varying amplitudes) indicated the presence of a third correlation time. From the obtained values of the amplitudes, it was difficult to identify the relationship between the amplitudes of the correlation times and the orientation angle α.

As described in the next section, the diffusion equation for a tilted dipole on the spherical surface was solved ex-

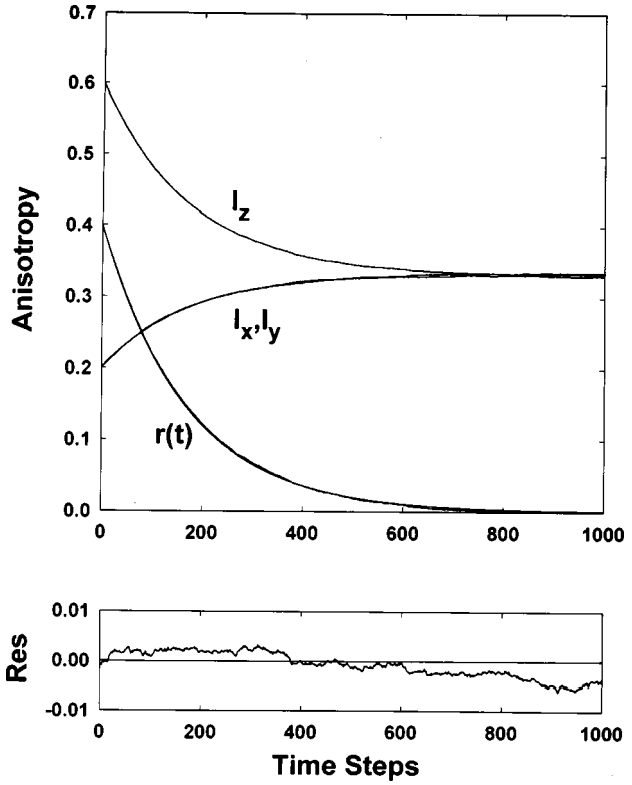

FIG. 5. Simulated fluorescence anisotropy decay, $r(t)$, due to the translational diffusion of dipoles oriented along the radial vectors on the surface of a sphere (see caption for Fig. 4). I_x, I_y, and I_z are the intensities along the three directions which were used to calculate $r(t)$ using Eq. (12). The decay was simulated for the values of the radius of the sphere, $R=10$ Å, translational diffusion coefficient, $D_{tr}=1\times10^{-5}$ cm^2/s and time step per iteration, $\tau=1$ ps. The number of iterations can be doubled to achieve the same level of anisotropy decay by reducing τ by 4 or by reducing D_{tr} by 4. The single exponential anisotropy decay for the calculated correlation time, $R^2/6D_{tr}=166.67$ ps is overlaid on the simulated curve of $r(t)$. Deviation of calculated and simulated values are shown in the bottom panel.

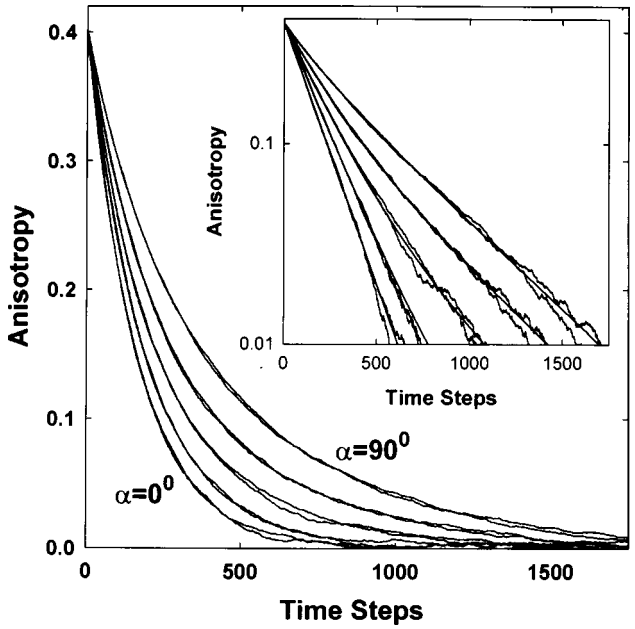

FIG. 6. Fluorescence anisotropy decays obtained from the Monte Carlo simulations of the translational diffusion of tilted dipoles on the surface of a sphere at different orientation angles $\alpha=0°$, 30°, 45°, 60°, and 90°, are shown. The decays were simulated for the values $R=10$ Å, $D_{tr}=1\times10^{-5}$ cm^2/s, and $\tau=1$ ps. The figure shows two decays for each value of α, simulated using different sets of random numbers. Inset shows the fits of these decays to Eq. (17), plotted on log scale.

actly. The anisotropy decay due to translational diffusion of tilted dipoles with an initial distribution as in the fluorescence experiment on the spherical surface is the sum of three exponentials,

$$r(t)=\tfrac{2}{5}(\cos^2\alpha-\tfrac{1}{2}\sin^2\alpha)^2\exp(-6D_{tr}t/R^2)+\tfrac{6}{5}\sin^2\alpha\cos^2\alpha\exp(-5D_{tr}t/R^2)+\tfrac{3}{10}\sin^4\alpha\exp(-2D_{tr}t/R^2). \quad (17)$$

The simulated anisotropy decays for different orientation angles α are fitted to the theoretical equation and the fits are shown in the inset of Fig. 6. The simulated decays fit well to the analytical equation indicating the correctness of the Monte Carlo method to simulate the translational diffusion on the sphere.

It may be noted that the coefficients of the exponentials in Eq. (17) are functions of α and the decay constants are functions of D_{tr}/R^2. For $\alpha=0°$, $r(t)=0.4\exp(-6D_{tr}t/R^2)$ which is the well known result for the fluorescence anisotropy due to rotational diffusion of a spherical solute in liquids[1] with the following equivalence between the rotational and translational diffusion coefficients: $D_{rot}=D_{tr}/R^2$. It may be noted also that the translational correlation time is $R^2/6D_{tr}$, not $R^2/4D_{tr}$ as assumed in interpreting the experimental fluorescence anisotropy decay data of fluorescent dyes in micelles.[6] For $\alpha=90°$, the decay is two exponential and more significantly, the slowest component, $(2D_{tr}/R^2)$, is predominant. The decay component with the decay constant $(5D_{tr}/R^2)$, is significant only at intermediate angles with maximum component at $\alpha=45°$. As explained in the next section, the origin of slow decay components is due to the geometric phase factor which arises due to the diffusion of a vectorial property on a spherical surface.

Although Eq. (17) contains three exponentials, there are only two fitting parameters, translational diffusion time τ_{tr} defined as R^2/D_{tr} and the orientation angle α, that have to be optimized in the analysis of the experimental data. Section III C describes the application of this equation in interpreting the anisotropy decay of a fluorescent probe embedded in micelles. Micelles are the smallest possible curved biological surfaces where the translational diffusion contributes significantly to the fluorescence depolarization during the lifetime of the excited fluorophore.

B. Analytical solution for the translational diffusion of oriented dipoles on a spherical surface

When the dipoles are oriented parallel to the radial vectors, the diffusion equation becomes the usual spherical harmonics equation[31] with the radial coordinate being a constant at the radius of the sphere, R,

$$\frac{\partial}{\partial t}P(\theta,\phi,t)=D_{tr}\nabla^2P(\theta,\phi,t), \quad (18)$$

where $P(\theta,\phi,t)$ is the probability of finding the dipole at the angular coordinates θ and ϕ at time t, ∇^2 is the Laplacian in the spherical polar coordinates. Here θ and ϕ represent the polar and azimuthal angles of the dipole, respectively. This equation can be easily separated into the two angular parts (θ and ϕ parts) using the method of separation of variables.[32] The θ part becomes

$$\frac{1}{R^2 \sin\theta}\frac{\partial}{\partial\theta}\left(\sin\theta\frac{\partial}{\partial\theta}\right)P(\theta,t) = -\frac{\lambda}{D_{\mathrm{tr}}}P(\theta,t). \tag{19}$$

The general solution which satisfy the above equation is

$$P(\theta,t) = \Sigma_l A_l P_l(\cos\theta)\exp\left(-\frac{l(l+1)D_{\mathrm{tr}}}{R^2}t\right), \tag{20}$$

where $P_l(\cos\theta)$ are the lth order Legendre Polynomial and A_l is the corresponding scaling factor.

In this case where the dipoles are oriented parallel to radial vectors, the fluorescence anisotropy equation is defined by

$$r(t) = \langle P_2(\cos\Omega)\rangle_t = \langle P_2(\cos\theta)\rangle_t, \tag{21}$$

where Ω is the angle made by the dipole with the z-axis. Using the above solution [Eq. (20)] for the θ part, the anisotropy equation becomes a single exponential as

$$r(t) = c\exp\left(-\frac{6D_{\mathrm{tr}}t}{R^2}\right), \tag{22}$$

where c is a constant. That means, the fluorescence anisotropy decays exponentially with a correlation time of $R^2/6D_{\mathrm{tr}}$ when the dipoles are oriented parallel to the radial vectors. This is in agreement with the Monte Carlo simulations.

The theoretical derivation of the fluorescence anisotropy equation becomes complex in the case where the dipoles are oriented at a particular angle α with the radial vectors. A diffusion equation similar to Eq. (18) has to be set up for the translational diffusion in such a case and has to be solved to obtain the solution similar to Eq. (20). The main difference that arises when $\alpha \neq 0$ is the geometric phase factor.[33,34] When the dipole is oriented at an angle with the respective radial vector, the direction at which the dipole points at a given time during the translational diffusion depends on the path it followed to arrive at that particular position. That means the phases of the different dipole vectors starting at the same initial position and arriving at the same final position but following different paths will be different. A recent study was focused on understanding the distribution of these geometric phases during the Brownian motion on a sphere.[35] This geometric phase factor has to be taken care of in setting up and solving the diffusion equation. This requires a different formalism which should include one extra degree of freedom which takes account the phase factor for the diffusion process on the surface of a sphere. This was done as follows.

For solving the problem of translational diffusion of oriented dipoles, we consider an additional frame associated with the dipole in addition to the space-fixed x, y, and z axes. Let an orthonormal set of three vectors **a**, **b**, and **c** be the frame attached with the dipole that is undergoing translational diffusion. The vector **c** is selected such that it is parallel to the radial vector and the dipole is tilted at an angle α with respect to **c** in the plane of the vectors **b** and **c**. Hence the unit dipole vector that is undergoing translational diffusion becomes $\mathbf{c}\cos\alpha + \mathbf{b}\sin\alpha$. The model for translational diffusion which was simulated here by the Monte Carlo methods gives this abc frame infinitesimal random rotations around the body fixed **a** and **b** axes. In this process, the **c** axis moves and with it the location of the dipole on the surface of the sphere. If **c** returns to its original value in this process of diffusion, the dipole has returned to the same point on the sphere, but because of the geometric phase effect discussed before, the **a** and **b** axes need not, in general, return to their original values, and hence the dipole will be different. By working on this formalism of two frames (space fixed and body fixed), we have ensured that the extra degree of freedom required to take account of the geometric phase factor is explicitly included.

With the excitation light polarized along the z-axis, the probability of excitation of the dipole located at **a**, **b**, **c** is equal to the square of the component of the dipole vector on the z-axis, i.e., $(c_z\cos\alpha + b_z\sin\alpha)^2$. After time t, let the dipole diffuse to $\mathbf{a}'$, $\mathbf{b}'$, $\mathbf{c}'$ with the probability $P(\mathbf{a}',\mathbf{b}',\mathbf{c}':\mathbf{a},\mathbf{b},\mathbf{c}:t)$. Projecting it back onto the space fixed z axis and squaring, the intensity I_z becomes

$$I_z \propto (c_z\cos\alpha + b_z\sin\alpha)^2(c_z'\cos\alpha + b_z'\sin\alpha)^2. \tag{23}$$

The expression for anisotropy can be written as

$$r(t) = \frac{3}{2}\frac{I_z(t)}{I(t)} - \frac{1}{2}, \tag{24}$$

where $I = I_x + I_y + I_z$ is the total fluorescence intensity.

For calculating $r(t)$, one needs to compute the ensemble average of I_z. That can be obtained by multiplying the expressions for I_z [Eq. (23)] and the probability P and integrating over **a**, **b**, **c** and $\mathbf{a}',\mathbf{b}',\mathbf{c}'$. The conditional probability P is the solution of the diffusion equation which at $t=0$ is a delta function centered around the initial frame. This is the Green's function of the diffusion equation. It can be expressed in a similar manner to the Green's function of the Schrodinger equation, in terms of eigenfunctions,

$$P(a',b',c':a,b,c:t) = \Sigma_p \Psi_p(a',b',c') \times \Psi_p(a,b,c)\exp(-E_p t). \tag{25}$$

Here Ψ_p, E_p are the eigenfunctions and eigenvalues, (labeled by the index p) of the corresponding diffusion operator.

For the case of interest, i.e., absence of rotation about the radial direction to the spherical surface, the diffusion operator will be proportional to $J_a^2 + J_b^2$. The absence of J_c^2 shows that we have built-in the constraint of no rotation about the normal to the sphere. This operator is similar to the Hamiltonian of the symmetric top molecule. Hence the eigenvalues and eigenfunctions will be similar to those which occur in the quantum-mechanical treatment of the symmetric top.[36] The appropriate quantum numbers are (i) J which enters the eigenvalue of the square of the angular momentum as $J(J+1)$, (ii) M, which is the eigenvalue of the z component of the angular momentum, i.e., along the space fixed z axis, and (iii) K which is the eigenvalue of the **c** component of angular

momentum, i.e., along the body fixed z axis. These three operators commute and their eigenvalues are sufficient to label states for the top, whose wave functions depend on three variables. The conventional choice for these three variables is the set of Euler angles giving the orientation of the body fixed frame with respect to the space fixed frame.[37] But for the problem considered here, it is convenient to use the components of **a**, **b**, and **c** which in turn can be expressed in terms of Euler angles. The intensity I_z is already expressed in terms of these components [Eq. (23)]. The eigenvalues of the diffusion operator $J_a^2+J_b^2$ are obtained by adding and subtracting J_c^2 (since $J^2=J_a^2+J_b^2+J_c^2$) and hence these are $J(J+1)-K^2$. Taking account of the angular diffusion coefficient D_{tr}/R^2, the eigenvalues of the diffusion equation becomes $(J(J+1)-K^2)D_{\mathrm{tr}}/R^2$.

Each of the factors in I_z can be expressed as a sum of eigenfunctions. This ensures that when I_z [Eq. (23)] is multiplied by P [Eq. (25)] and integrated to compute the average of I_z over the ensemble, only those eigenfunctions will contribute and the rest will disappear by the orthogonality relations. The four relevant eigenfunctions are

$$\Psi_0=1,$$

$$\Psi_1=\sqrt{\tfrac{45}{4}}(c_z^2-1/3),$$

$$\Psi_2=\sqrt{15}b_z c_z,$$

and

$$\Psi_3=\sqrt{\tfrac{15}{4}}(b_z^2-a_z^2). \tag{26}$$

The eigenfunction Ψ_0 corresponds to that of the quantum numbers $J=0$, $M=0$, and $K=0$ and have the zero eigenvalue. The three eigenfunctions Ψ_1, Ψ_2, and Ψ_3 have $J=2$, and $M=0$, but have different $|K|$ values as 0, 1, 2, and hence the corresponding eigenvalues are 6, 5, and 2.

One of the factors in the intensity expression [Eq. (23)] can be written as

$$\begin{aligned}(c_z\cos\alpha+b_z\sin\alpha)^2=&\sqrt{\tfrac{4}{45}}(\cos^2\alpha-\tfrac{1}{2}\sin^2\alpha)\Psi_1\\&+\sqrt{\tfrac{4}{15}}(\sin\alpha\cos\alpha)\Psi_2\\&+\sqrt{\tfrac{1}{15}}\sin^2\alpha\Psi_3+\tfrac{1}{3}\Psi_0.\end{aligned} \tag{27}$$

The constant term (Ψ_0 term) corresponds to the nondecaying term under diffusion (zero eigenvalue). The second factor in I_z can be similarly written in terms of primed quantities. Multiplying I_z by P and integrating over the initial and final parameters of the frame, the expression for I_z was obtained as the sum of the squares of the coefficients of eigenfunctions in Eq. (27). It can be calculated that $I=\frac{1}{3}$ and is independent of α and time. Hence the anisotropy r can be computed as

$$\begin{aligned}r(t)=&\frac{2}{5}\left(\cos^2\alpha-\frac{1}{2}\sin^2\alpha\right)^2\exp\left(\frac{-6D_{\mathrm{tr}}t}{R^2}\right)\\&+\frac{6}{5}\sin^2\alpha\cos^2\alpha\exp\left(\frac{-5D_{\mathrm{tr}}t}{R^2}\right)\\&+\frac{3}{10}\sin^4\alpha\exp\left(\frac{-2D_{\mathrm{tr}}t}{R^2}\right).\end{aligned} \tag{28}$$

The constant $J=0$ term cancels against the $-\frac{1}{2}$ in the expression for $r(t)$ [Eq. (24)].

This is the expression tested in Sec. III A against the results obtained from the Monte Carlo simulations of the translational diffusion of oriented dipoles on the surface of a sphere. At zero time, $r(t)$ takes the value 0.4 independent of α [Eq. (28)], as expected. The slower decays occur only if α is nonzero. Although the translational diffusion is happening with the same diffusion coefficient, the depolarization of the fluorescence anisotropy is slower for the case of dipoles oriented away from the normal to the spherical surface because of the presence of nonzero $|K|$ modes of diffusion. For the case of the dipole normal to the sphere, only $K=0$ contributes, and the equation for the time resolved fluorescence anisotropy is $\exp(-6D_{\mathrm{tr}}t/R^2)$ which can also be obtained more simply from the eigenvalue $l(l+1)$ of the Laplacian on the sphere, for $l=2$ [Eqs. (18) and (20)].

C. Diffusion of Nile red in SDS micelles

SDS micelles were prepared by stirring the surfactant solution at a concentration above the critical micellar concentration (cmc) of 8 mM in warm deionized water for about 1 h. SDS micelles prepared thus are known to be spherical (core radius of approximately 16.7 Å) and the aggregation number is ≈ 62.[8,38,39] Nile red being a hydrophobic molecule it is insoluble and nonfluorescent in water.[40] It solubilizes readily in SDS micelles.[8] The distribution of the dye among micelles is governed by Poisson statistics. At a low concentration ratio of the dye to micelle used in the experiments (2.27 μM of dye and 0.99 mM of micelle) the probability of finding more than one dye per micelle is extremely small, i.e., $<0.2\%$.[8] The fluorescence is therefore from the dye molecules that are present as one per micelle. The fluorescence decay of Nile red in SDS collected at the emission maximum is single exponential with a lifetime of 2.53 ns. The G-factor corrected parallel ($F_\parallel$) and perpendicular ($F_\perp$) components of fluorescence are shown in Fig. 7(A). Figure 7(B) shows the smooth polarized intensity decays ($I_\parallel$ and $I_\perp$) obtained by fitting the fluorescence curves to the convolution equation [Eq. (13)] as described in the Methods. The anisotropy decay, $r(t)$ obtained using Eq. (15) is shown in Fig. 8.

The fluorescence anisotropy decay of fluorophores embedded in micelles and its origin in terms of molecular dynamics have been studied and discussed.[6,7] The fluorescence anisotropy decay for the dye molecule in a spherical micelle is caused by three independent depolarizing motions: (i) the translational motion of the dye on the spherical surface of the micelle, (ii) wobbling dynamics of the dye about the local symmetry axis in the micelle,[41,42] and (iii) the rotational dynamics of the spherical micelle as a whole. The decay time

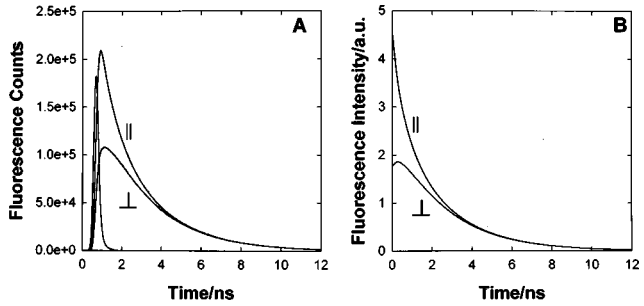

FIG. 7. (A) *G*-factor corrected experimental polarized fluorescence decays ($F_{\parallel}$ and $F_{\perp}$ components) of Nile red in SDS micelles. The instrument response function, $R(t)$ is also shown in the figure. (B) Polarized intensity decays ($I_{\parallel}$ and $I_{\perp}$) obtained by deconvoluting the fluorescence decays using the convolution integral [Eq. (13)] using $R(t)$ and a four exponential function for $I_{\parallel}$ and $I_{\perp}$. The fitted equations were $I_{\parallel}(t)=0.6267\exp(-t/0.2690\ \text{ns})+1.1976\exp(-t/0.8059\ \text{ns})+1.5506\exp(-t/2.4798\ \text{ns})+1.1865\exp(-t/2.4825\ \text{ns})$, and $I_{\perp}(t)=-0.7636\exp(-t/0.5035\ \text{ns})+0.9712\exp(-t/2.5463\ \text{ns})+0.9193\exp(-t/2.5471\ \text{ns})+0.6532\exp(-t/2.5473\ \text{ns})$.

constants associated with the three motions are τ_{tr} (translational diffusion), τ_w (wobbling dynamics) and τ_m (rotation of the micelle). These three motions are shown in Fig. 9. As described earlier, the fluorescence anisotropy decay due to translational diffusion on the spherical surface is given by Eq. (17). The mathematical equations for the fluorescence anisotropy decay due to wobbling dynamics and rotation of the micelle are as follows.

The fluorescence anisotropy due to the wobbling dynamics of a linear molecule in a planar membrane is generally described in terms of the wobbling-in-a-cone model where the molecule wobbles within a cone of semiangle θ_0 that is related to the order of the environment.[41,42] According to this model, the anisotropy decay equation becomes

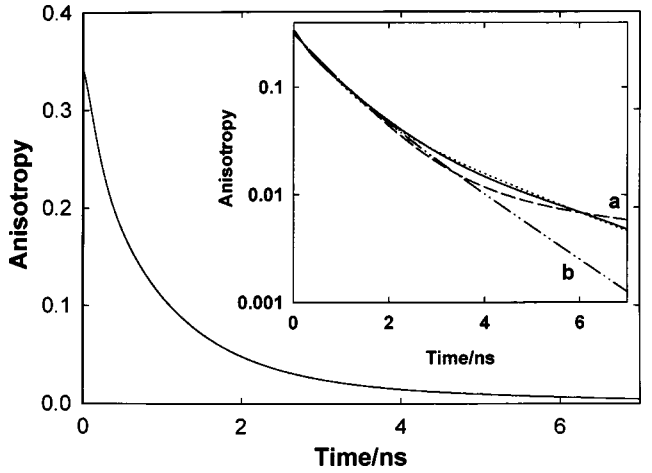

FIG. 8. Fluorescence anisotropy decay of Nile red in SDS micelles, generated using the polarized fluorescence intensity decays that are shown in the Fig. 7(B). The inset shows the fitting of this anisotropy decay to different models, plotted on log scale. The solid curve is the experimental anisotropy decay. The dashed (curve a) and dashed–dotted (curve b) curves are the fits to Eq. (33) with $S=1$ (no wobbling dynamics) and with $D_{\text{tr}}=0$ (no translational diffusion). The dotted curve overlapping with the experimental curve shows the fitting to Eq. (33) that includes all the three depolarizing motions for $S=0.471$ (see text for details).

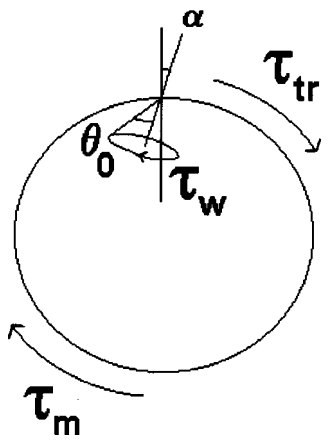

FIG. 9. The three depolarizing motions for the fluorescent probe in a micelle; (i) wobbling dynamics of the dye in the micelle (τ_w), (ii) the lateral diffusion of the dye on the surface of the micelle (τ_{tr}), and (iii) the rotational diffusion of the spherical micelle (τ_m). τ_w, τ_{tr}, and τ_m are the decay constants that can be associated with the physical parameters related to the three processes, respectively.

$$\frac{r(t)}{r(0)}=[S^2+(1-S^2)\exp(-t/\tau_w)], \tag{29}$$

where S is the order parameter and τ_w is the wobbling time constant. The order parameter S is related to the cone semiangle θ_0 according to the equation

$$S=\tfrac{1}{2}(\cos\theta_0)(1+\cos\theta_0). \tag{30}$$

Wobbling dynamics of the dye molecule in micelle may be considered similar to that in the membrane. The wobbling time constant τ_w is related to the wobbling diffusion constant D_w by the relation (according to the wobbling-in-cone model[42]),

$$\begin{aligned}D_w\tau_w(1-S^2)=&-x_0^2(1+x_0)^2[\log[(1+x_0)/2]\\&+(1-x_0)/2]/[2(1-x_0)]\\&+(1-x_0)(6+8x_0-x_0^2-12x_0^3-7x_0^4)/24,\end{aligned} \tag{31}$$

where $x_0=\cos\theta_0$.

The rotational motion of the spherical micelle leads to a single exponential anisotropy decay,

$$\frac{r(t)}{r(0)}=\exp\left(-\frac{t}{\tau_m}\right), \tag{32}$$

where τ_m is the rotational time constant for the spherical micelle. τ_m is calculated to be 8.3 ns in water at 25 °C using the Stokes–Einstein equation, $\tau_m=\eta V/kT$, where V is the molecular volume of the micelle [hydrodynamic radius, $r_H=21$ Å (Refs. 8,13)] and η is the viscosity.[8] This value was kept constant in the data analysis to fit $r(t)$ which is described below.

The three motions described above which depolarize the fluorescence are independent of each other and hence the anisotropy decay is the multiplication of the three parts as given below,

$$\frac{r(t)}{r(0)}=\left[\left(\cos^2\alpha-\frac{1}{2}\sin^2\alpha\right)^2\exp\left(\frac{-6t}{\tau_{\mathrm{tr}}}\right)+3\sin^2\alpha\cos^2\alpha\exp\left(\frac{-5t}{\tau_{\mathrm{tr}}}\right)+\frac{3}{4}\sin^4\alpha\exp\left(\frac{-2t}{\tau_{\mathrm{tr}}}\right)\right]\times[S^2+(1-S^2)\exp(-t/\tau_w)]\exp\left(-\frac{t}{\tau_m}\right). \quad (33)$$

Here, τ_{tr} represents the translational diffusion time which is defined as R^2/D_{tr}, where R is the radius of the micelle and D_{tr} is the translational diffusion coefficient.

The experimental anisotropy decay shown in Fig. 8 was initially fitted (using Jandel Scientific Sigmaplot V. 3.0) by assuming that the translational diffusion is absent; that is, $D_{\mathrm{tr}}=0$ in Eq. (33). The best fit (curve a in Fig. 8) for this equation was obtained for $S=0.2$ and $\tau_w=1.01$ ns. Clearly, neglecting the translational diffusion leads to a misfit of experimental data.

Next, the effect of neglecting wobbling dynamics was examined by setting $S=1$ in Eq. (33). The best fit values for α and τ_{tr} were 63.01° and 3.54 ns but the fit was unsatisfactory as seen by the deviation of the fitted curve (curve b in Fig. 8) from the data. Thus, it is necessary to include both wobbling and translational diffusion in the equation. This required optimization of four unknown parameters in Eq. (33), namely, S, τ_w, α, and D_{tr}. The experimental data of $r(t)$ was fitted to Eq. (33) by optimizing these four parameters. It was found that the optimized values for the four parameters varied substantially. The range for each of these parameters was obtained from the fits as $S=0.60\pm0.16$, $\tau_{\mathrm{tr}}=15.26\pm9.14$ ns, $\alpha=0.36\pm37.52°$, and $\tau_w=0.73\pm0.19$ ns. In order to determine these parameters accurately, it was decided to make use of the value of order parameter S determined by an independent method (see below) as a fixed parameter.

SDS micelles swell to a large size in the presence of NaCl and form large wormlike/rodlike micelles at high salt and surfactant concentrations.[39,43–45] Because of the large size, τ_{tr} and τ_m are also large compared to fluorescence lifetime and hence these contributions in Eq. (33) are absent. Hence, the order parameter S can be determined in this case from the ratio of the fluorescence anisotropy at zero time (r_0) and the limiting value at long time (r_∞) as $S=(r_\infty/r_0)^{0.5}$ (Refs. 42, 46 and 47). Highly viscous micelles containing the dye were prepared by mixing the dye (1.73 mM) with the concentrated solution of the surfactant (1.73 M, dye to surfactant ratio of 1:1000) and then drying the solution on a glass plate until it became a film of thick paste. The anisotropy decay was obtained for this film by placing the glass plate at an angle of 45° to the exciting laser beam. From the values of r_0 (0.365) and r_∞ (0.081), the order parameter S was calculated to be 0.471.

The experimental anisotropy decay data of Nile red in SDS micelles was fitted to Eq. (33) by fixing the value of S at 0.471. The best fit values were $\alpha=0.98\pm1.91°$, $\tau_{\mathrm{tr}}=21.89\pm0.48$ ns, and $\tau_w=0.89\pm0.01$ ns. Figure 8 shows the best fit curve (dotted curve) overlapping with the experimental curve. From the values of τ_{tr} and the core radius of the micelle $R=16.7$ Å,[8,38] the translational diffusion coefficient was calculated to be $1.27\pm0.03\times10^{-10}$ m^2/s. The wobbling diffusion coefficient was calculated to be $2.10\pm0.02\times10^8$ s^{-1} using the values of S and τ_w and Eq. (31). From the value of S, the cone semiangle θ_0 (Refs. 41, 42) was calculated to be 53.7°.

The application of Eq. (33) to interpret the experimental anisotropy decay for Nile red in SDS micelles has given good estimates for the value of the tilt angle of the molecular dipoles as $1°\pm2°$. From this value, one may consider that the molecular dipoles are aligned parallel to the radial direction. However, the molecule wobbles in a cone of large semiangle of 53.7° indicating considerable mobility for the dye molecule. The values of the different parameters obtained above using a fixed value of S are only indicative since S was obtained from a different system and viscosity dependence, if any, has not been included in the analysis. Also, in deriving the expression for the anisotropy decay of the system, the anisotropy is written as the product of the three terms as contributions from the three independent motions in the case of the micelle [refer to Eq. (33)]. The rotational motion of the micelle is independent of the molecular dynamics of the probe and hence it can be decoupled from the other two motions. On the other hand, the decoupling of the wobbling (rotation) and translational motion of the molecule is assumed in liquid solutions which may not be valid for molecules in interfaces. Indeed, there exists enough experimental evidence, the so-called ''translation rotation paradox,''[48] or non-Brownian dynamics[8] to suggest that the decoupling may not be correct. On the other hand, the uncoupling of the translational and wobbling diffusions may be valid when the time scales of these two motions differ substantially which is the case here as can be seen from the obtained values of the two time constants. The method employed here also gives estimates for the wobbling diffusion coefficient D_w and translational diffusion coefficient D_{tr}. Fluorescence anisotropy dynamics in micelles and the analysis of data is perhaps unique because one obtains values for D_w and D_{tr} in a single experiment. There is however no independent method by which the accuracy of these values can be checked. On the other hand, the values of the translational and wobbling diffusion coefficients compare reasonably well with those reported for organic molecules in micelles and membranes.[8,6,12,13,49–52]

It is interesting to speculate on the possible use of the experimental and simulation methods described in this paper for a quantitative understanding of the characteristics of the surface of irregular objects of small size such as proteins and biological membranes. The fluorescence anisotropy decay of a fluorophore which is noncovalently bound to the surface of the protein would have contributions from translational diffusion and rotation of the entire surface. Unlike micelles, the probe cannot intercalate into the protein and hence the wobbling dynamics is absent except in the case of covalently linked fluorophores. The analysis of experimental data becomes simple if experiments are designed such that rotation of the protein is prevented by immobilization. In which case, the anisotropy decay is purely because of the lateral diffusion of the fluorophore on the surface of the protein. The surface characteristics of the protein and the tilt angle of the probe

are contained in the fluorescence anisotropy decay. The size and shape of the protein can be determined only by comparison with the theoretical equations for regular shapes (sphere, ellipsoid, etc.) or simulated functions (for irregular shapes) for fluorescence anisotropy. If there are regions in the surface of the protein (for example, the active site) which are forbidden for the lateral diffusion of the fluorophore then one expects that anisotropy does not decay to zero but to a constant value which is proportional to the excluded area. Some knowledge of the shape and size of the protein will be helpful in such cases to carry out Monte Carlo simulation and to obtain quantitative data on excluded area. In the case of fluorescence dynamics in lipid bilayer vesicles, the contribution of translational diffusion is negligible to the total fluorescence depolarization because of the larger values of R and the timescales of observation (nanoseconds). However, the equations derived here will really hold good in the case of phosphorescence or NMR and ESR measurements on lipid vesicles where the phosphorescence lifetimes or spin relaxation times that are measured are in the order of microseconds to milliseconds and the translational diffusion on a vesicle surface significantly affects these parameters.[14]

The Monte Carlo simulations carried out here to simulate the diffusion of tilted dipoles on the surface of a sphere clearly show that the anisotropy decay due to translational diffusion depends on the orientation of the dipoles on curved surfaces. The equations derived here apply as well in the case of NMR and ESR studies in understanding the mechanisms behind the millisecond or microsecond relaxation times of probes in biological membranes or in any experimental study that measures the translational diffusion of a vectorial property on curved surfaces. The orientation factor is an important factor to be considered, that has not got much attention in literature, in explaining the fluorescence anisotropy decay of fluorescent probes on curved biological surfaces.

The Monte Carlo simulations described in this paper can be generalized for application to the diffusion of oriented dipoles on any curved surface. The simulations will be of use, particularly, in those systems which cannot be treated analytically. Based on the geometry of the surface, the simulation procedure described here for the case of a sphere can be easily modified. In the case of complicated curved surfaces, position dependent probability equations can be used to simulate the diffusion process.

IV. SUMMARY

Monte Carlo simulations were used to simulate the translational diffusion of oriented dipoles on a sphere. The anisotropy decay is single exponential for the special case of dipoles oriented along the radial direction. The simulated decays agreed well with the three exponential equation for the anisotropy decay obtained by solving the diffusion equation for this problem. The decay time constants are $R^2/6D_{\mathrm{tr}}$, $R^2/5D_{\mathrm{tr}}$, and $R^2/2D_{\mathrm{tr}}$, where R is the radius of the sphere and D_{tr} is the translational diffusion coefficient. The preexponential factors are functions of the orientation angle made by the dipoles with the normal to the sphere.

Fluorescence anisotropy decay of molecules intercalated in nanometer size spherical micelles has contributions from three independent dynamical motions; translational diffusion as described above, wobbling of the molecular axis spanning a cone (wobbling-in-cone model), and rotation of the spherical micelle. The anisotropy decay obtained from experimentally determined polarized fluorescence responses of Nile red in SDS micelles was fitted to the theoretical equation [Eq. (33)] which required optimization of the values for τ_{tr}, τ_w, and α. Nile red in SDS micelles is oriented at $1\pm2°$ with the normal to the micellar surface and the translational diffusion coefficient is estimated to be $1.3\pm0.1\times10^{-10}$ m^2/s.

ACKNOWLEDGMENTS

The authors thank Dr. S. N. Mazumdar and Professor Deepak Dhar for the discussions regarding the analytical solution for the translational diffusion of oriented dipoles.

[1] G. R. Fleming, *Chemical Applications of Ultrafast Spectroscopy* (Oxford University Press, New York, 1986).
[2] W. W. Mantulin and G. Weber, J. Chem. Phys. **66**, 4092 (1977).
[3] R. L. Christensen, R. C. Drake, and D. Philips, J. Phys. Chem. **90**, 5960 (1986).
[4] U. K. A. Klein and H. P. Haar, Chem. Phys. Lett. **58**, 531 (1978).
[5] A. J. W. G. Visser, K. Vos, A. V. Hoek, and J. S. Santema, J. Phys. Chem. **92**, 759 (1988).
[6] E. L. Quitevis, A. H. Marcus, and M. D. Fayer, J. Phys. Chem. **97**, 5762 (1993).
[7] N. C. Maiti, S. Mazumdar, and N. Periasamy, J. Phys. Chem. **99**, 10708 (1995).
[8] N. C. Maiti, M. M. G. Krishna, P. J. Britto, and N. Periasamy, J. Phys. Chem. B **101**, 11051 (1997).
[9] B. W. Van der Meer, K. H. Cheng, and S. Y. Chen, Biophys. J. **58**, 1517 (1990).
[10] S. Y. Chen, K. H. Cheng, B. W. Van der Meer, and J. M. Beechem, Biophys. J. **58**, 1527 (1990).
[11] S. Y. Chen, K. H. Cheng, and B. W. Van der Meer, Biochemistry **31**, 3759 (1992).
[12] H. Walderhaug, O. Soederman, and P. Stilbs, J. Phys. Chem. **88**, 1655 (1984).
[13] H. Nery, O. Soederman, C. D. , H. Walderhaug, and B. Lindman, J. Phys. Chem. **90**, 5802 (1986).
[14] P. W. Kuchel, A. J. Lennon, and C. Durrant, J. Magn. Reson. **112**, 1 (1996).
[15] M. G. Brereton and C. Butler, J. Phys. A **20**, 3955 (1987).
[16] D. C. Khandekar and F. W. Wiegel, J. Phys. (London) A **21**, L563 (1988).
[17] *Geometric Phases in Physics*, edited by A. Shapere and F. Wilczek (World Scientific, Singapore, 1989).
[18] S. Sinha and J. Samuel, Phys. Rev. B **50**, 13871 (1994).
[19] J. Crank, *The Mathematics of Diffusion* (Oxford University Press, London, 1956).
[20] P. R. Bevington and D. K. Robinson, *Data Reduction and Error Analysis for the Physical Sciences*, 2nd ed. (McGraw–Hill, New York, 1994).
[21] W. H. Press, S. A. Teukolsky, W. T. Vetterling, and B. P. Flannery, *Numerical Recipes in C: The Art of Scientific Computing*, 2nd ed. (Cambridge University Press, Cambridge, 1992).
[22] L. Jansen and M. Boon, *Theory of Finite Groups. Application in Physics: Symmetry Groups of Quantum Mechanical Systems* (North–Holland, Amsterdam, 1967).
[23] S. Chandrasekhar, Rev. Mod. Phys. **15**, 1 (1943).
[24] N. Periasamy, S. Doraiswamy, G. B. Maiya, and B. Venkataraman, J. Chem. Phys. **88**, 1638 (1988).
[25] K. V. Bankar, V. R. Bhagat, R. Das, S. Doraiswamy, A. S. Ghangrekar,

D. S. Kamat, N. Periasamy, V. J. P. Srivatsavoy, and B. Venkataraman, Indian J. Pure Appl. Chem. **27**, 416 (1989).
[26] A. Grinvald and I. Z. Steinberg, Anal. Biochem. **59**, 583 (1974).
[27] D. V. O'Connor and D. Philips, *Time Correlated Single Photon Counting* (Academic, London, 1984).
[28] R. F. Steiner, ''Fluorescence anisotropy: Theory and applications,'' in *Topics in Fluorescence Spectroscopy*, edited by J. R. Lakowicz (Plenum, New York, 1991), Vol. 2, p. 1.
[29] G. B. Dutt, S. Doraiswamy, N. Periasamy, and B. Venkataraman, J. Chem. Phys. **93**, 8498 (1990).
[30] A. J. Cross and G. R. Fleming, Biophys. J. **46**, 45 (1984).
[31] A. Abragam, *The Principles of Nuclear Magnetism* (Oxford University Press, London, 1961).
[32] E. Kreyszig, *Advancesd Engineering Mathematics*, 7th ed. (Wiley, New York, 1993).
[33] R. Nityananda, Curr. Sci. **67**, 238 (1994).
[34] J. W. Zwanziger, M. Koenig, and A. Pines, Annu. Rev. Phys. Chem. **41**, 601 (1990).
[35] M. M. G. Krishna, J. Samuel, and S. Sinha, ''Brownian motion on a sphere: Distribution of solid angles'' (unpublished).
[36] L. D. Landau and E. M. Lifshitz, *Quantum Mechanics: Nonrelativistic Theory*, 3rd ed. (Pergamon, Oxford, 1977).
[37] C. H. Townes and A. L. Schawlow, *Microwave Spectroscopy* (McGraw–Hill, New York, 1955).
[38] C. Tanford, J. Phys. Chem. **76**, 3020 (1972).
[39] K. Kalyanasundaram, *Photochemistry in Microheterogeneous Systems* (Academic, New York, 1991).
[40] D. L. Sacket and J. Wolff, Anal. Biochem. **167**, 228 (1987).
[41] K. J. Kinosita, S. Kawato, and A. Ikegami, Biophys. J. **20**, 289 (1977).
[42] G. Lipari and A. Szabo, Biophys. J. **30**, 489 (1980).
[43] N. A. Mazer, G. B. Benedek, and M. C. Carey, J. Phys. Chem. **80**, 1075 (1976).
[44] M. J. Rosen, *Surfactants and Interfacial Phenomena*, 2nd ed. (Wiley, New York, 1989).
[45] C. Tanford, *The Hydrophobic Effect: Formation of Micelles and Biological Membranes*, 2nd ed. (Wiley, New York, 1980).
[46] M. P. Heyn, FEBS Lett. **108**, 359 (1979).
[47] F. Jahnig, Proc. Natl. Acad. Sci. USA **76**, 6361 (1979).
[48] D. B. Hall, A. Dhinojwala, and J. M. Torkelson, Phys. Rev. Lett. **79**, 103 (1997).
[49] M. Ameloot, H. Hendrickx, W. Herreman, H. Pottel, F. V. Cauvelaert, and W. Van der Meer, Biophys. J. **46**, 525 (1984).
[50] S. Wang, J. M. Bechem, E. Gratton, and M. Glaser, Biochemistry **30**, 5565 (1991).
[51] C. D. Stubbs and B. W. Williams, ''Fluorescence in Membranes,'' in *Topics in Fluorescence Spectroscopy*, edited by J. R. Lakowicz (Plenum, New York, 1992), Vol. 3, p. 231.
[52] A. Haibel, G. Nimtz, R. Pelster, and R. Jaggi, Phys. Rev. E **57**, 4838 (1998).